International Journal of Power Electronics and Drive System (IJPEDS)
Vol. 5, No. 3, February 2015, pp. 293~304
ISSN: 2088-8694

FPGA-Based Implementation Direct Torque Control of Induction Motor

Saber KRIM[1], Soufien GDAIM[2], Abdellatif MTIBAA[3], Mohamed Faouzi MIMOUNI[4]
[1,2,3]Laboratory of Electronics and Microelectronics (EuE), Faculty of Sciences of Monastir
University of Monastir, Tunisia
[4]Research Unit of industrial systems Study and renewable energy (ESIER),
University of Monastir, Tunisia.
[3,4]Department of Electrical Engineering, National Engineering School of Monastir, University of Monastir, Tunisia

Article Info

Article history:

Received Aug, 2014
Revised Jan 13, 2015
Accepted Jan 28, 2015

Keyword:

Direct Torque Control
Induction Motor
Field Programmable Gate Array
Real Time
Sliding mode observer
VHDL
Xilinx System Generator

ABSTRACT

This paper proposes a digital implementation of the direct torque control (DTC) of an Induction Motor (IM) with an observation strategy on the Field Programmable Gate Array (FPGA). The hardware solution based on the FPGA is caracterised by fast processing speed due to the parallel processing. In this study the FPGA is used to overcome the limitation of the software solutions (Digital Signal Processor (DSP), Microcontroller...). Also, the DTC of IM has many drawbacks such as for example; The open loop pure integration has from the problems of integration especially at the low speed and the variation of the stator resistance due to the temperature. To tackle these problems we use the Sliding Mode Observer (SMO). This observer is used estimate the stator flux, the stator current and the stator resistance. The hardware implementation method is based on Xilinx System Generator (XSG) which a modeling tool developed by Xilinx for the design of implemented systems on FPGA; from the design of the DTC with SMO from XSG we can automatically generate the VHDL code. The model of the DTC with SMO has been designed and simulated using XSG blocks, synthesized with Xilinx ISE 12.4 tool and implemented on Xilinx Virtex-V FPGA.

Corresponding Author:

Saber KRIM,
Laboratory of Electronics and Microelectronics (EuE), Faculty of Sciences of Monastir,
National Engineering School of Monastir, University of Monastir, Tunisia
E-mial: krimsaber@hotmail.fr

1. INTRODUCTION

With technological advancement in the field of microelectronics new digital solutions such as FPGAs (Field Programmable Gate Array) or ASIC (Application Specific Integrated Circuit) are available and can be used as numerical targets for the implementation of algorithms command. The inherent parallelism of these digital solutions and their high calculation capacity make the calculation time is negligible in spite of the complexity of the algorithms to be implanted. These hardware solutions can meet the new demands of modern controls, such as reduction of the calculation time, the processing parallelism of these hardware solutions allows integrating on a single target several algorithms that provide various features and which can work independently of each other. For the control of the variable speed electrical machines, various control algorithms can be used. These algorithms often have several nested control loops. In our case we use the DTC that contains a speed control loop, stator flux regulator, electromagnetic torque regulator and the sliding mode observer; this is why we are interested in the implementation on FPGA of Direct Torque Control based on the sliding mode observer for controlling an induction motor. During the past few years several researchers use the FPGA for controlling electrical system [1]-[7]. Most of them develop the algorithm on a VHDL hardware description language. For the hardware implementation of the Directe Torque Control with

Sliding Mode Observer of an induction motor on the FPGA we use Xilinx System Generator (XSG) toolbox developed by Xilinx and added to matlab/simulink. The XSG advantages are the rapid time to market, real time and portability. Once the design and simulation of the proposed algorithme is completed we can automatically generate the VHDL code in Xilinx ISE.

The DTC of IM is based on the orientation of the stator flux by a direct action on the states of the switches of the inverter [8]-[11]. The DTC control based on an open loop estimator of stator flux having well-known problems of integration especially at a low speed [12]-[14]; also, it is sensitive to the variation of the machine parameters such as stator resistance [15]. To solve these problems many observation methods are used, such as the Extended Kalman Filter [16] but the drawback of this observer that the knowledge of load dynamics is not usually possible, Model Reference Adaptive System (MRAS) [17], [18]; the drawback of this algorithm that it is sensitive to uncertainties of the induction motor parameters, the luenberger Observer is used for state estimation of IM [19]. In this work, we propose to use the adaptive sliding mode observer for the estimation of the stator flux, stator current and the adaptation of the variation of the stator resistance. That is a powerful observer that can estimate simultaneously the stator flux, stator current, rotor speed and motor parameters. It is introduced to replace the open-loop estimator of stator flux. Furthermore it has been provided with an adaptation mechanism of the stator resistance. Thus, the aim of this paper is first, to give a fair comparison between a DTC with an open loop estimator and DTC with sliding mode observer at the stage of adjustment of the stator resistance. Secondly, the proposed model is developed using Xilinx System Generator for implementation on FPGA, to enjoy the performances of FPGAs in the field of digital control of electrical machines in real time. The performance of the proposed model is proved by simulation results, Resources used and execution time.

2. DIRECT TORQUE CONTROL OF AN INDUCTION MOTOR

2.1. Induction Machine Model

The state model of an induction machine can be expressed as follows:

$$\frac{dX}{dt} = [A]X + [B]U \tag{1}$$

Where A, B, X and U are the evolution matrix, the control matrix, state vector X and the stator voltage respectively.

$$[A] = \begin{pmatrix} -\frac{\frac{R_S}{L_S}+\frac{R_r}{L_r}}{\sigma} & -\omega & \frac{R_r}{\sigma L_r L_S} & \frac{\omega}{\sigma L_S} \\ \omega & -\frac{\frac{R_S}{L_S}+\frac{R_r}{L_r}}{\sigma} & -\frac{\omega}{\sigma L_S} & \frac{R_r}{\sigma L_r L_S} \\ -R_S & 0 & 0 & 0 \\ 0 & -R_S & 0 & 0 \end{pmatrix}, [B] = \begin{pmatrix} \frac{1}{\sigma * L_S} & 0 \\ 0 & \frac{1}{\sigma * L_S} \\ 1 & 0 \\ 0 & 1 \end{pmatrix}, X = \begin{pmatrix} i_{s\alpha} \\ i_{s\beta} \\ \varphi_{s\alpha} \\ \varphi_{s\beta} \end{pmatrix}, U = \begin{pmatrix} V_{s\alpha} \\ V_{s\beta} \end{pmatrix}$$

The state vector X is composed by stator current and flux components. The vector command U is constituted by the stator voltage components.

2.2. Direct Torque Control Principle

Direct torque control of an induction machine is based on the direct determination of the control sequence applied to the switches of a voltage inverter. The choice of sequences is based on the two hysteresis comparators of the stator flux and electromagnetic torque [20]. The voltage vector Vs is the output of a three-phase voltage inverter whose the state of the inverter switches are controlled by three Boolean variables Sj (j = a, b, c). The voltage vector can be written as:

$$\begin{cases} V_S = \sqrt{\frac{2}{3}} U \left(S_a + S_b . e^{j\frac{2\pi}{3}} + S . e^{j\frac{4\pi}{3}} \right) \\ \overline{v}_s = v_{s\alpha} + j v_{s\beta} \end{cases} \tag{3}$$

The components of the stator voltage vector $V_S\left(V_{S\alpha}, V_{S\beta}\right)$ and the stator flux vector $\varphi_S\left(\varphi_{S\alpha}, \varphi_{S\beta}\right)$ in Concordia reference are given by Equation (4) and (5). The calculation of the position and module of the stator flux are based on the use of components $\left(\varphi_{S\alpha}, \varphi_{S\beta}\right)$. The module of the stator flux and its position are given by Equation (6).

$$\begin{cases} \varphi_{s\alpha} = \int_0^t (v_{s\alpha} - R_s i_{s\alpha})dt \\ \varphi_{s\beta} = \int_0^t (v_{s\beta} - R_s i_{s\beta})dt \end{cases} \quad (4)$$

$$\begin{cases} V_{S\alpha} = \sqrt{\frac{2}{3}}U\left(Sa - \frac{1}{2}(Sb + Sc)\right) \\ V_{S\beta} = \sqrt{\frac{2}{3}}U\left(Sb - Sc\right) \end{cases} \quad (5)$$

$$\begin{cases} \varphi_s = \sqrt{\varphi_{s\alpha}^2 + \varphi_{s\beta}^2} \\ \theta_S = \arg\varphi_s = arctg\dfrac{\varphi_{s\beta}}{\varphi_{s\alpha}} \end{cases} \quad (6)$$

The electromagnetic torque is expressed in terms of the components of stator flux vector and the components of stator current vector as:

$$C_e = \frac{3}{2}p(\varphi_{s\alpha}i_{s\beta} - \varphi_{s\beta}i_{s\alpha}) \quad (7)$$

The estimated values of the stator flux and electromagnetic torque are compared with their reference values Φsref, Teref respectively. Switching states are selected by the switching table, where E_C is the error of electromagnetic torque after hysteresis block and E_φ is the error of the stator flux after hysteresis block, $S_i(i = 1...6)$ means the sector (Table 1) [21]:

Table 1. Switching table for direct torque control

Eφ	*Ec*	S1	S2	S3	S4	S5	S6
1	1	V2	V3	V4	V5	V6	V1
	0	V7	V0	V7	V0	V7	V0
	-1	V6	V1	V2	V3	V4	V5
0	1	V3	V4	V5	V6	V1	V2
	0	V0	V7	V0	V7	V0	V7
	-1	V5	V6	V1	V2	V3	V4

The structure of DTC of an induction motor is given, as shown by the Figure 1:

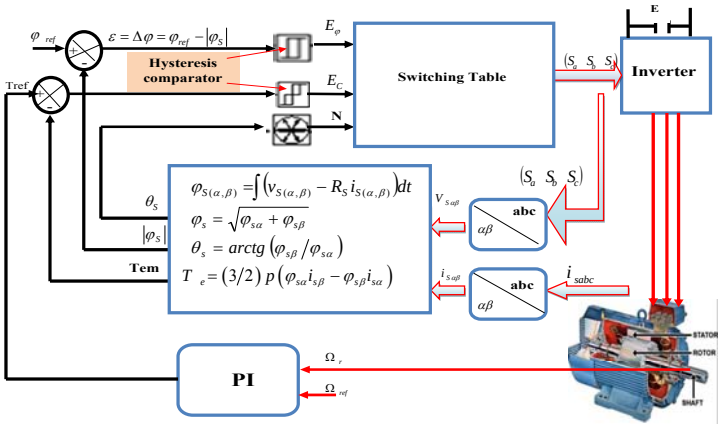

Figure 1. Schematic of conventional DTC

3. DIRECT TORQUE CONTROL OF AN INDUCTION MOTOR WITH SLIDING MODE OBSERVER

The sliding mode observer (SMO) is wedely used for non linear systems due to its robustness to the parameter variations. The SMO is used to contstruct the state variables and the stator resistance. The diagram of the SMO is shown in Figure 2.

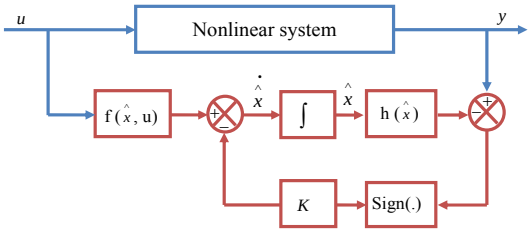

Figure 2. Principle of the sliding mode observer

The mathematical model of the observed stator current is presented as:

$$\begin{pmatrix} \dot{\hat{i}}_{S\alpha} \\ \dot{\hat{i}}_{S\beta} \end{pmatrix} = \begin{pmatrix} -\frac{1}{\sigma}\left(\frac{R_S}{L_S}+\frac{R_r}{L_r}\right) & -\omega \\ \omega & -\frac{1}{\sigma}\left(\frac{R_S}{L_S}+\frac{R_r}{L_r}\right) \end{pmatrix} \begin{pmatrix} \hat{i}_{S\alpha} \\ \hat{i}_{S\beta} \end{pmatrix} + \begin{pmatrix} \frac{R_r}{\sigma L_r L_S} & \frac{\omega}{\sigma L_S} \\ -\frac{\omega}{\sigma L_S} & \frac{R_r}{\sigma L_r L_S} \end{pmatrix} \begin{pmatrix} \hat{\varphi}_{S\alpha} \\ \hat{\varphi}_{S\beta} \end{pmatrix} + \begin{pmatrix} \frac{1}{\sigma * L_S} & 0 \\ 0 & \frac{1}{\sigma * L_S} \end{pmatrix} \begin{pmatrix} v_{S\alpha} \\ v_{S\beta} \end{pmatrix} + \begin{pmatrix} A_{11} & A_{12} \\ A_{21} & A_{22} \end{pmatrix} \begin{pmatrix} I_{S1} \\ I_{S2} \end{pmatrix} \quad (8)$$

The matimatical model of the observed stator flux is given by the following system:

$$\begin{pmatrix} \dot{\hat{\varphi}}_{S\alpha} \\ \dot{\hat{\varphi}}_{S\beta} \end{pmatrix} = \begin{pmatrix} -R_S & 0 \\ 0 & -R_S \end{pmatrix} \begin{pmatrix} \hat{i}_{S\alpha} \\ \hat{i}_{S\beta} \end{pmatrix} + \begin{pmatrix} \frac{1}{\sigma * L_S} & 0 \\ 0 & \frac{1}{\sigma * L_S} \end{pmatrix} \begin{pmatrix} v_{S\alpha} \\ v_{S\beta} \end{pmatrix} + \begin{pmatrix} A_{31} & A_{32} \\ A_{41} & A_{42} \end{pmatrix} \begin{pmatrix} I_{S1} \\ I_{S2} \end{pmatrix} \quad (9)$$

Where:

$\begin{pmatrix} A_{11} & A_{12} \\ A_{21} & A_{22} \end{pmatrix}$, $\begin{pmatrix} A_{31} & A_{32} \\ A_{41} & A_{42} \end{pmatrix}$ and $\begin{pmatrix} I_{S1} \\ I_{S2} \end{pmatrix} = \begin{bmatrix} signe(S_1) \\ signe(S_2) \end{bmatrix}$: are the matrixes of gains of the observed stator current, matrix of gains of the observed stator flux, and the sign vector of the sliding mode surface respectively.

3.1. Determining of the SMO Characteristics

The sliding surface is based on the error between the real stator current $i_{s\alpha}$ and $i_{s\beta}$, and the observed stator current $\hat{i}_{s\alpha}$ and $\hat{i}_{s\beta}$ as follows:

$$S = \begin{bmatrix} S_1 \\ S_2 \end{bmatrix} = \frac{1}{\sigma L_S (\frac{1}{T_r^2} + \omega^2)} \begin{bmatrix} \frac{1}{T_r} & -\omega \\ \omega & \frac{1}{T_r} \end{bmatrix} \begin{bmatrix} i_{s\alpha} - \hat{i}_{s\alpha} \\ i_{s\beta} - \hat{i}_{s\beta} \end{bmatrix} \quad (10)$$

Where: $i_s = \begin{bmatrix} i_{s\alpha} & i_{s\beta} \end{bmatrix}^T$ and $\hat{i}_s = \begin{bmatrix} \hat{i}_{s\alpha} & \hat{i}_{s\beta} \end{bmatrix}^T$ are the real and observed stators currents vectors respectively.

$T_r = \frac{L_r}{R_r}$: Rotor time constant.

The matrix of gains related to the current observer is as follows:

$$A_i = \begin{bmatrix} A_{i1} & A_{i2} \\ A_{i3} & A_{i4} \end{bmatrix} = \Gamma \begin{bmatrix} \delta_1 & 0 \\ 0 & \delta_2 \end{bmatrix} \quad (11)$$

Where $\delta_1 \, and \, \delta_2$ are two positive constants, which are determined by applying the stability conditions defined by the Lyapunov approach.

The gain matrix of the stator flux is as follows:

$$A_\varphi = \begin{bmatrix} A_{\varphi 1} & A_{\varphi 2} \\ A_{\varphi 3} & A_{\varphi 4} \end{bmatrix} = \begin{bmatrix} q_1 \delta 1 & \frac{\omega}{\sigma L_S} \\ -\frac{\omega}{\sigma L_S} & q_2 \delta_2 \end{bmatrix} \quad (12)$$

Where $q_1 \, and \, q_2$ are two positive constants.

The stability of the SMO depends on its convergence towards its sliding surface. To study the stability of this observer the following Lyapunov function is used:

$$V = \frac{1}{2} S^T S \quad (13)$$

When the sliding surface S=0, the error between the real and observed stator current must bee zero, $i_{s\alpha} - \hat{i}_{s\alpha} = 0$ and the derivate of the lyapunov fuction is strictly negative ($\dot{V} \prec 0$).

$$\dot{V} = S^T \dot{S} \prec 0 \quad (14)$$

The major drawback of the SMO observer is the chattering phenomenon. To weaken this phenomenon a saturation function is used to replace the Bang-Bang function. The saturation function is given by the system (15).

$$sign\ (S_i) = \begin{cases} 1 & si \quad S_i > \lambda \\ -1 & si \quad S_i < -\lambda \\ \frac{S_i}{\lambda} & si \quad |S_i| < \lambda \end{cases} \quad ; i = 1,2 \quad (15)$$

Where λ is a positive constant with a low value.

3.2. Mechanism of Adaptation of the Stator Resistance

During operation the stator résistance vary, due to the temperature and the low speed operation. To online estimate of the stator resistance another term added to the lyapunov fuction.

$$V = \frac{1}{2} S^T S + \frac{\lambda}{2}\left(\hat{R}_S - R_S \right)^2 \tag{16}$$

$$\dot{V} = S^T \dot{S} + \lambda\left(\hat{R}_S - R_S \right)\dot{\hat{R}}_S \prec 0 \tag{17}$$

To satisfy the condition of the Equation (17), the estimated stator resistance can be expressed as follow:

$$\dot{\hat{R}}_S = -k\left(\hat{i}_{S\alpha} * (i_{S\alpha} - \hat{i}_{S\alpha}) + \hat{i}_{S\beta} * (i_{S\beta} - \hat{i}_{S\beta}) \right) \tag{18}$$

With k is a positive constant.

4. USE OF XILINX SYSTEM GENERATOR (XSG) IN THE CONTROLLER DESIGN

4.1. Description of Xilinx System Generator

Xilinx System Generator (XSG) is a modeling tool developed by Xilinx for the design of implemented systems on FPGA. It has a library of varied blocks, which can be automatically compiled into an FPGA [22]. In this work, Xilinx System Generator (XSG) is used to implement the architecture of the Direct Torque Control of induction Motor with sliding mode observer on FPGA. In the first step, we begin by implementing of the proposed architectures using the XSG blocks available on the Simulink library. Once the Design of the system is completed and gives the desired simulation results, the VHDL code can be generated by the XSG tool [23]. The design flow of the Xilinx System Generator is given by figure 3. After generation of VHDL code and the synthesis, we can generate the bitstream file. Then we can move this configuration file to program the FPGA [24].

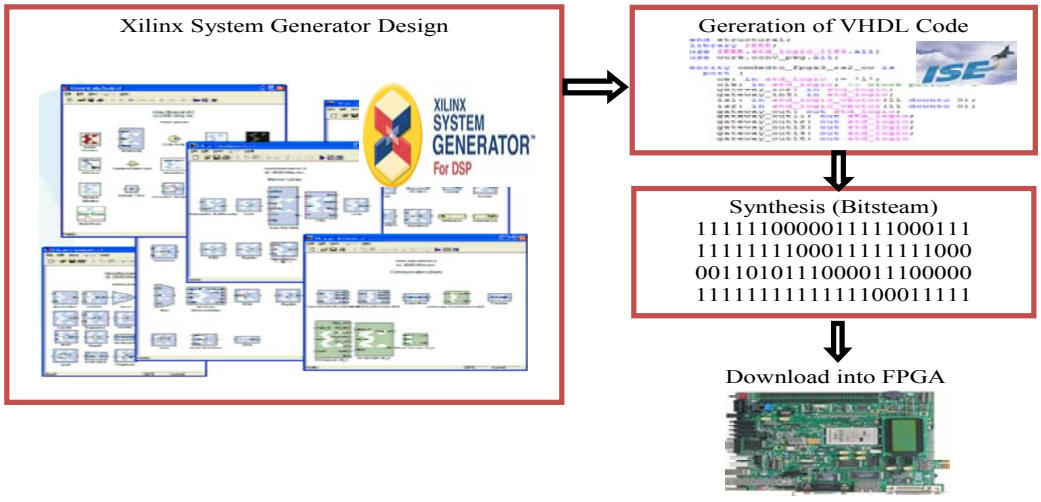

Figure 3. Configuring an FPGA

4.2. Design of the Sliding Mode Observer using XSG

4.2.1. Design of the Currents Observed

The Design of the direct component of the observed stator current vector introduced into the equation system (8) given by Figure 4.

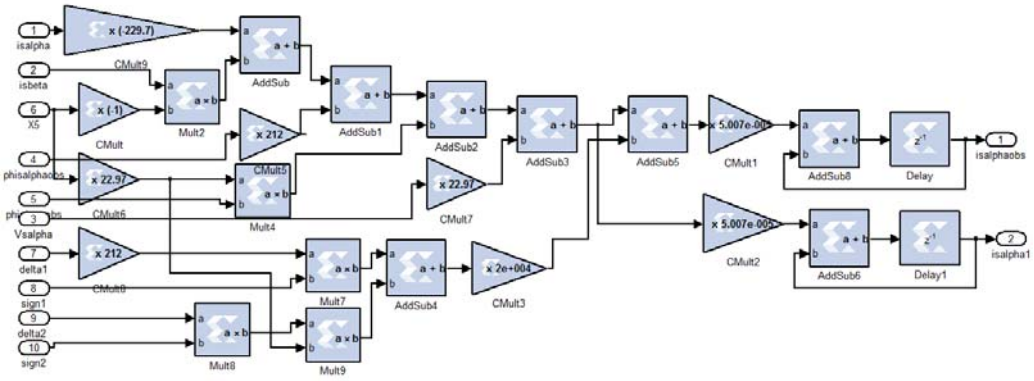

Figure 4. Design of the Component $\hat{i}_{S\alpha}$ from the XSG

4.2.2. Design of Sliding Surface, gain Matrix and Sign Function

The sliding surface, the saturation function and the gain matrix are given in equations (10), (11), (12) and (15), are illustrated using XSG as shown in Figure 5.

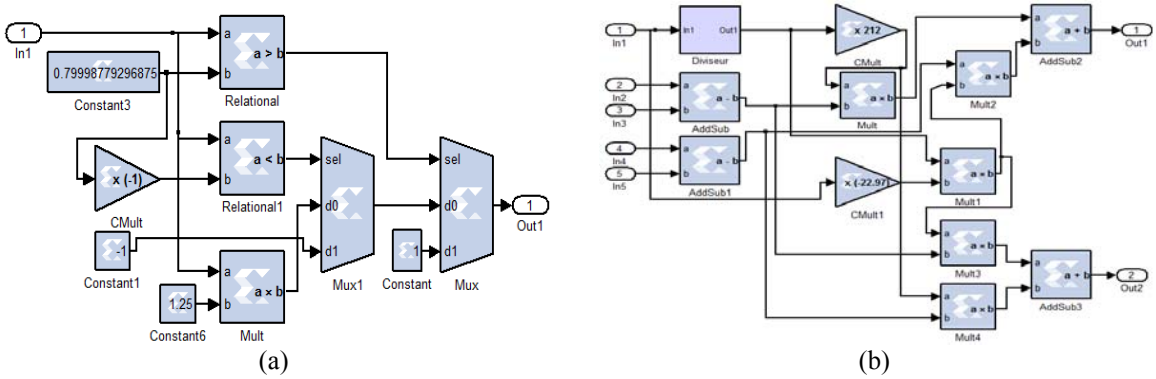

Figure 5. Design of sliding surface, gain matrix and sign function from the XSG

4.3. Simulation Results using Xilinx System Generator and Discussions

The structure of the direct torque control with the adaptative sliding mode observer of an induction motor is shown in Figure 6.

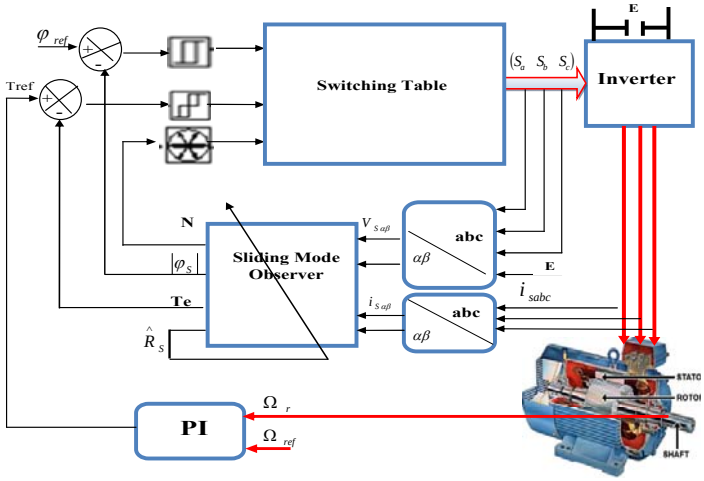

Figure 6. Schematic of a conventional DTC with an adaptative sliding mode observer

4.3.1. The Stator Resistance is Constant (Rs=5.717Ω)

The simulation of the conventional DTC with sliding mode observer is achieved using the XSG. The speed and flux references used in the simulation results are 150rad/s and 0.91wb respectively. The electromagnetic torque reference presents the output of PI controller of speed. At time t = 0.5sec a load torque of 10 Nm is applied.

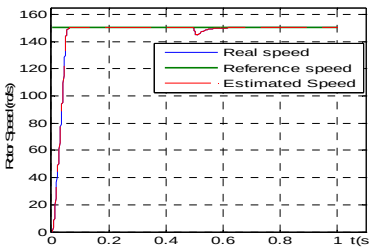

(a)

Figure 7(a). Evolution of real and estimated speed

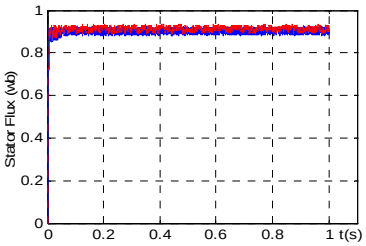

(b)

Figure 7(b). Evolution of the real and observed stator flux

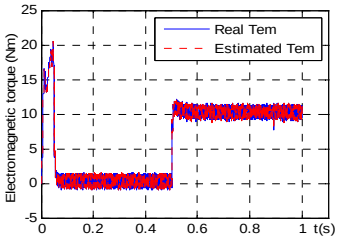

(c)

Figure 7(c). Evolution of the real and estimated electromagnetic torque

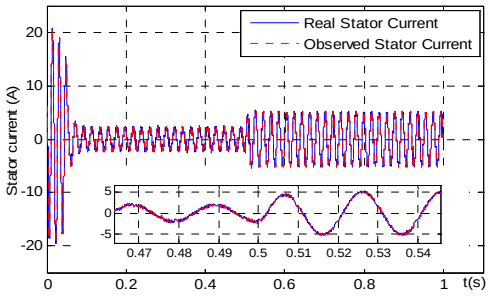

Figure 8(a). Variation of the real and observed stator current $\hat{i}_{S\alpha}$

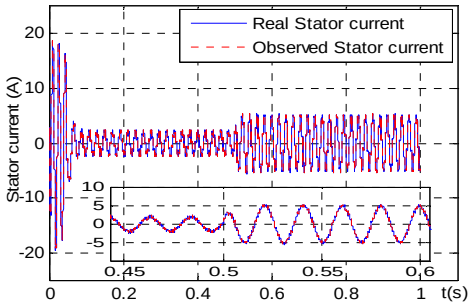

Figure 8(b): Variation of the observed and real stator current $\hat{i}_{S\beta}$

4.3.2. The Stator Resistance Varies from 100% (Rs=2*5.717=11.434Ω)

The simulation of the conventional DTC with an open loop estimator and the conventional DTC with a sliding mode observer is achieved using the XSG at a low speed. The rotor speed and stator flux references used in the simulation results are 31.4 rad/s and 0.91 wb, respectively. At time t = 0.2sec a load torque of 10 Nm is applied. At t = 0.4sec the stator resistance increases by 100%.

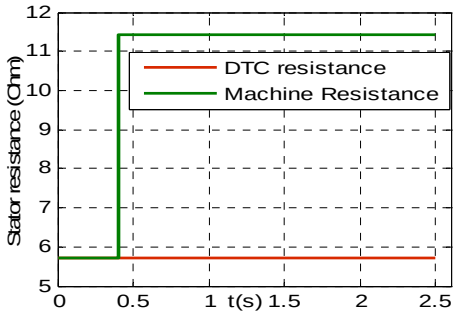

(a) An open loop estimator

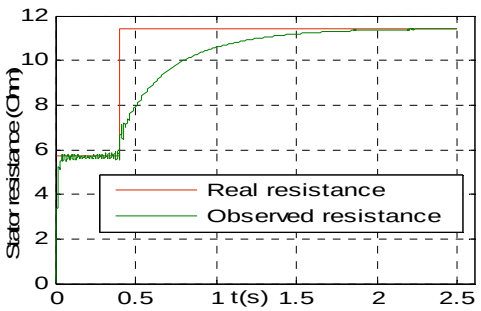

(b) A sliding mode observer

Figure 9. Variation of Rs for DTC with

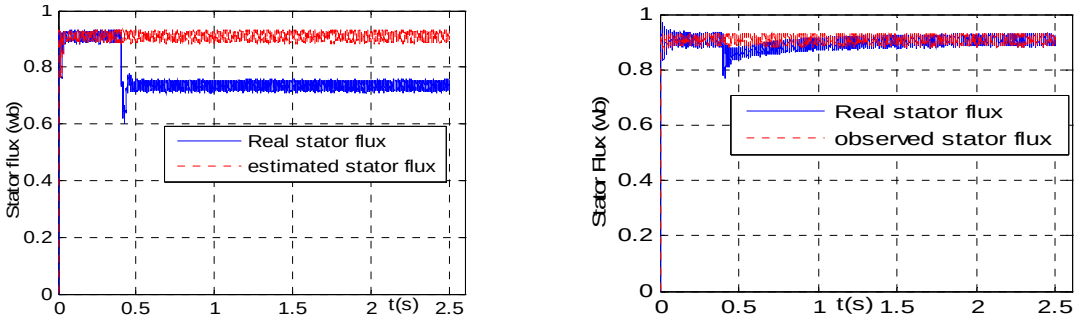

(a) An open loop estimator (b) With a sliding mode observer

Figure 10. Evolution of the stator flux for DTC with

(a) without adjustment of the stator resistance variation (b) with adjustment of the stator resistance variation

Figure 11. Evolution of the stator flux trajectories

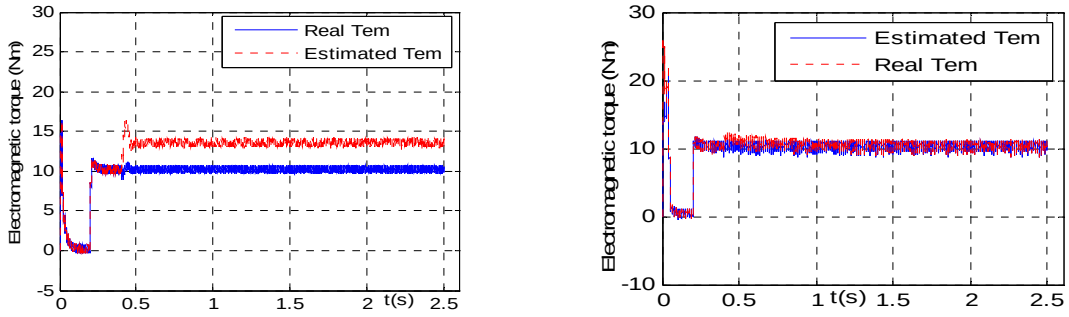

(a) An open loop estimator (b) With a Sliding Mode Observer

Figure 12. Variation of electromagnetic torque for DTC with

The simulation results of the direct torque control with sliding Mode Observer given by Figure 7 and 8 show that the real and the estimated variables are similar. In Figure 7(b) and 7(c) it can be seen that the stator flux and the electromagnetic torque are characterized by high ripples due to the use of the hysteresis comparator.

Figure 9 show the sensitivity of the Direct Torque Control of an Induction Motor. In Figure 9(a) we can see at t=0.4sec that the stator resistance increases 2 times the nominal stator resistance due to temperature, it can be seen that in the case of the DTC with an open loop estimator, the stator resistance used in the DTC kept constant. By contrast, in Figure 9(b) the observed stator resistance converges rapidly to the nominal value, this is due to the on line adaptation of the stator resistance by the sliding mode observer. The simulation results demonstrates the robustness of the Sliding Mode Observer against the abruptly variation of the machine parametres.

In Figure 10(a), at t = 0.4sec the real stator flux is affected by de variation of the stator resistance, it decreases abruptly to 0.72 wb, the error between the real and the reference stator flux kept constant. Yet, in

the Figure 10(b), the static error gradually vanishes due to the presence of the adaptive online mechanism of the stator resistance using the Sliding Mode Observer.

In Figure 11(a), we can notice that the stator flux trajectories increase due to the variation of the stator resistance at t=0.4sec. By contrast, in Figure 11(b) the stator flux trajectory is kept constant due to the presence of the adaptive online mechanism of the stator resistance using the Sliding Mode Observer.

In Figure 12(a), at t = 0.4sec the electromagnetic torque increases, and the error between the electromagnetic torque and the load torque remains constant. However, in Figure 12(b), for the sliding mode observer; the electromagnetic torque is kept constant.

4.4. FPGA Implementation Results of the Proposed Approach and Discussions

Once the simulation is completed and gives the desired results, we can generate the VHDL code and synthesized the hardware block. The implementation results are given by Figure 13 and Table 2.

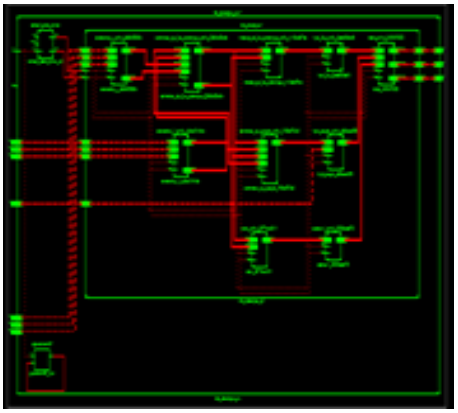

Figure 13(a). RTL schematic of the conventional DTC with a sliding mode observer from Xilinx ISE

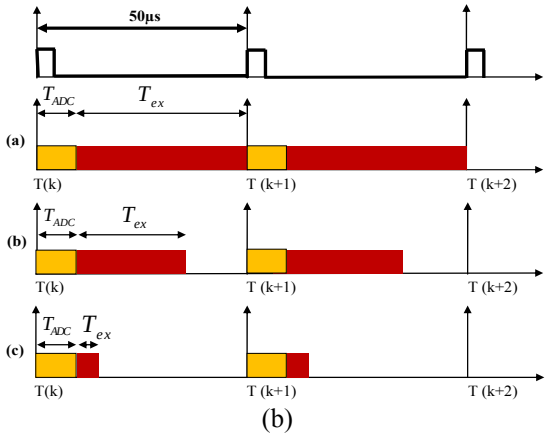

Figure 13(b). Timing Diagram for the Imlementation on (a): Microcontroller, (b): Digital Signal Processor (DSP), (c): Field Programmable Gate Array (FPGA)

Table 2. Resources Utilisation for the DTC with SMO

Resourses	Used resources	Available resources
Number of bonded I/O	68	640
Number of Slice LUTs	2087	44800
Number of Slices Registers	478	44800
Number of DSP48Es	8	128
Execution time: T_{ex} = 0.94 µs		

The Table 2 shows the implementation results in term of the used resources and the execution time of the Direct Torque Control with SMO using the FPGA Virtex-5 Device. The RTL schematic of the CDTC with SMO is given by Figure 13(a). The Figure 13(b), shows the performance of computing time for the hardware implementation on FPGA compared to software solutions (Microcontroller, Digital Signal Processor). T_{ADC} and T_{ex} are the analogue to digital conversion time and the execution time respectively.

In this work the execution time equal to 0.94 µs. But in papers [25] and [26], the sampling time equal to 100 µs using the dSPACE 1104 (digital signal processing and control engineering). In paper [27], the sampling time equal to 500 µs. It can be seen that the execution time is too important relative to the FPGA due to the sequential processing of the dSPACE.

5. CONCLUSION

In this paper, the digital implementation of the Direct Torque Control with Sliding Mode Observer using the FPGA has been presented. The Sliding mode Observer has been proposed to improve the

performences of the Direct Torque Control of an Induction Motor. Using the Sliding Mode Observer consists to remplacing the open loop pure integration. The simulations results using Xilinx System Generator have shown that the proposed observation strategy has better performances than the open loop pure integration especially in term of variation of the stator resistance. The obtained design of the Direct Torque Control with Sliding Mode Observer from XSG can be translated automatically into a VHDL (VHSIC Hardware Description Language) from Xilinx Integrated Software Environment tool (ISE) and can be embedded into the Xilinx Virtex-V FPGA.

Induction Machine Parameters

Number of pairs of poles: 2	Rotor resistance: 4,282 Ω	Mutual inductance :441,7mH
Rated frequency: 50 Hz	Stator inductance :464mH	Moment of inertia :0.0049 kg.m²
Rated voltage :220/380 V	Rotor inductance :464mH	Viscous friction coefficient: 0.0029kg.mˆ2/s
Stator resistance :5,717 Ω		

REFERENCES

[1] HM Hasanien. *FPGA implementation of adaptative ANN controller for speed regulation of permanent stepper motor drives*. Energy Conversion and Management. Elsevier Publisher. 2011

[2] E Monmasson, L Idkhajine, MN Cirstea, I Bahri, A Tisan, MW Naouar. FPGAs in Industrial Control Applications. *IEEE Transactions on Industrial Informatics*. 2011; 7(2): 224-243.

[3] M Dagbagi, L Idkhajine, E Monmasson, I.Slama-Belkhodja. *FPGA Implementation of Power Electronic Converter Real-Time Model.* International Symposium on Power Electronics, Electrical Drives, Automation and Motion. 2012; 658 – 663.

[4] E MONMASSON, I BAHRI, L IDKHAJINE, A MAALOUF, MW NAOUAR. *Recent Advancements in FPGA-based controllers for AC Drives Applications.* 13th International Conference on Optimization of Electrical and Electronic Equipment (OPTIM), IEEE. 2012; 8-15.

[5] M Shahbazi, P Poure, S Saadate, MR Zolghadri. FPGA-Based Reconfigurable Control for Fault-Tolerant Back-to-Back Converter without Redundancy. *IEEE Transactions on Industrial Electronics*. 2013; 60(8): 3360 - 3371.

[6] K Jezernik, J Korelic, R Horvat. PMSM Sliding Mode FPGA-Based Control for Torque Ripple Reduction. *IEEE Transactions on Power Electronics*. 2013; 28(7): 3549 - 3556.

[7] T Sutikno, NR Idris, A Jidin, MN Cirstea. An Improved FPGA Implementation of Direct Torque Control for Induction Machines. *IEEE Transactions on Industrial Informatics*. 2013; 9(3): 1272–1279.

[8] P Bibhu, P Dinkar, S Sabyasachi. A Simple hardware realization of switching table based direct torque control of induction motor. *Electric Power Systems research. Elsevier Publisher*. 2007; 77(2): 181-190.

[9] GS Buja, MP Kazmierkowski. Direct torque control of PWM inverter-fed AC motors-A survey. *IEEE Transactions on Industrial Electronics*, 2004; 51(4): 744-757.

[10] P Vas. Sensor less Vector and Direct Torque Control. Oxford University Press, London. 1998.

[11] I Takahashi, Y Ohmori. High-performance Direct Torque Control of an Induction Motor. *IEEE Transactions on Industry Applications*. 1989; 25(2): 257-264.

[12] R Rajendran, Dr N Devarajan. A Comparative Performance Analysis of Torque Control Schemes for Induction Motor Drives. *International Journal of Power Electronics and Drive System (IJPEDS).* 2012, 2(2): 177~191.

[13] M Barut, S Bogosyan, M Gokasan. Speed sensorless direct torque control of IMs with rotor resistance estimation. *International Journal Energy Conv. and* Manag. 2005; 46(3): 335-349.

[14] D Casadei, F Profumo, G Serra, A Tani, "FOC and DTC: Two Viable Schemes for Induction Motors Torque Control. *IEEE Transaction on Power Electronics*, 2002; 17(5): 779 – 787.

[15] S Meziane, R Toufouti, H Benalla. Speed Sensorless Direct Torque Control and Stator Resistance Estimator of Induction Motor Based MRAS Method. *International Journal of Applied Engineering Research (IJAER).* 2008; 3(6): 733-747.

[16] M Messaoudi, H Kraiem, M Ben Hamed, L Sbita, MN Abdelkrim. A Robust Sensorless Direct Torque Control of Induction Motor Based on MRAS and Extended Kalman Filter. *Leonardo Journal of Sciences*, 2008; 7(12): 35-56.

[17] Cirrincione M, Pucci M. Sensorless direct torque control of an induction motor by a TLS-based MRAS observer with adaptive integration. *Automatica*, 2005; 41(11): 1843-1854.

[18] MK Metwally. Control of Four Switch Three Phase Inverter Fed Induction Motor Drives Based Speed and Stator Resistance Estimation. *International Journal of Power Electronics and Drive System (IJPEDS).* 2014; 4(2): 192-203.

[19] Sbita L, Ben Hamed M. An MRAS–based full order Luenberger observer for sensorless DRFOC of induction motors. *Int. J. ACSE*, 2007; 7(1): 11-20.

[20] MM Rezaei, M Mirsalim. Improved Direct Torque Control for Induction Machine Drives based on Fuzzy Sector Theory. *Iranian Journal of electrical and Electronic Engineering*, 2010; 6(2): 110-118.

[21] A Mahfouz, WM Mamadouh. Intelligent DTC for PWSM Drive using ANFIS technique. *International Journal of Engineering Science and Technology (IJEST),* 2012; 4(3): 1208-1222.

[22] XSG, 1998. Xilinx system generator v2.1 basic tutorial. Printed in USA, http://bwrcs.eecs.berkeley.edu/Classes/cs152/handouts/Tutorials_book.pdf.

[23] JG Mailloux. Prototypage Rapide de la Commande Vectorielle sur FPGA à l'Aide des Outils SIMULINK SYSTEM GENERATOR, l'Université de Québec, Mars 2008.
[24] White paper: Using System Generator for Systematic HDL Design, Verification, and Validation WP283. 2008. (v1.0)
[25] Bhoopendra Singh, Shailendra Jain, Sanjeet Dwivedi. Direct Torque Control Induction Motor Drive with Improved Flux Response. *Hindawi Publishing Corporation Advances in Power Electronics.* 2012, Article ID 764038: 1-11.
[26] A ELBACHA, Z BOULGHASOUL, E ELWARRAKI. A Comparative Study of Rotor Time Constant Online Identification of an Induction Motor Using High Gain Observer and Fuzzy Compensator. *WSEAS TRANSACTIONS on SYSTEMS and CONTROL*. 2012; 7(2): 37-53.
[27] M Boussak, K Jarray. A High-Performance Sensorless Indirect Stator Flux Orientation Control of Induction Motor Drive. *IEEE Transactions on industrial electronics.* 2006; 53(1): 14-49.

BIOGRAPHIES OF AUTHORS

Saber KRIM received the degree in Electrical Engineering from National School of Engineering of Monastir, Tunisia in 2011. In 2013 he received his M.S degree in electrical Engineering from Monastir University, Tunisia. He is currently pursuing the Ph.D. degree with University of Monastir, Tunisia. His current research interests include rapid prototyping and reconfigurable architecture for real-time control applications of electrical system.

Soufien GDAIM received the degree in Electrical Engineering from National School of Engineering of Sfax, Tunisia in 1998. In 2007 he received his M.S degree in electronic and real-time informatic from Sousse University and received his PhD degree in Electrical Engineering in 2013 from ENIM, Tunisia. His current research interests include rapid prototyping and reconfigurable architecture for real-time control applications of electrical system.

Abdellatif MTIBAA is currently Professor in Micro-Electronics and Hardware Design with Electrical Department at the National School of Engineering of Monastir and Head of Circuits Systems Reconfigurable ENIM-Group at Electronic and microelectronic Laboratory. He holds a Diploma in Electrical Engineering in 1985 and received his PhD degree in Electrical Engineering in 2000. His current research interests include System on Programmable Chip, high level synthesis, rapid prototyping and reconfigurable architecture for real-time multimedia applications. Dr. Abdellatif Mtibaa has authored/coauthored over 100 papers in international journals and conferences. He served on the technical program committees for several international conferences. He also served as a co-organizer of several international conferences.

Mohamed Faouzi Mimouni received his Mastery of Science and DEA from ENSET, Tunisia in 1984 and 1986, respectively. In 1997, he obtained his Doctorate Degree in Electrical Engineering from ENSET, Tunisia. He is currently Full Professor of Electrical Engineering with Electrical Department at the National School of Engineering of Monastir. His specific research interests are in the area Power Electronics, Motor Drives, Solar and Wind Power generation. Dr. Med Faouzi MIMOUNI has authored/coauthored over 100 papers in international journals and conferences. He served on the technical program committees for several international conferences.